Analysis of Surface Plasmon-Polariton Modes with Metallic Structures and Polarized Light across Gapped Plasmonic Waveguides

Guhwan Kim, Sung-Ryoung Koo and Myung-Hyun Lee*
Department of Electrical and Computer Engineering, Sungkyunkwan University, Suwon, 16419, South Korea

Keywords: Surface Plasmon Polariton, Plasmonic Waveguide, Plasmonic Signal.

Abstract: We analyzed output Surface Plasmon-Polariton (SPP) modes with gold structures in a gap when polarized light propagated across Gapped SPP Waveguides (G-SPPWs). The G-SPPWs consist of input and output insulator-metal-insulator typed SPPWs with a gap. The dielectric channel waveguide is laid across the gap. Gold was used as the metal of the SPPWs. Low loss polymers were used as the upper and lower cladding layers and the core of the dielectric channel waveguide, respectively. The input SPP mode intersects at the gap with the polarized light launched to the dielectric channel waveguide. When the TE polarized light is applied, lossy short-range SPP (SRSPP) modes are overlapped in the output SPPW. For the TM polarized light, the output SPP mode has low loss though there are mode fluctuations. When horizontal and vertical gold strips are placed in the gap and the TE polarized light is applied, the propagation loss increases significantly depending on the shape of the gold strips due to TE-induced symmetric surface charges. Inverted plasmonic signals can be generated from optical signals by the SPP modulation using excited SRSPP modes. The modulation efficiency can be increased by introducing photonic crystal or plasmonic resonance in the gap.

1 INTRODUCTION

To accommodate the ever-increasing amount of data traffic, dielectric-based photonic devices have been introduced owing to the tremendous data carrying capacity and far faster-operating speed than electronic devices. However, it is hard to integrate relatively large photonic devices and nano-scaled electronic devices on the same dimension due to the fact that the scale of the dielectric photonic devices is limited to about half of the wavelength by the diffraction limit of light. Plasmonics can offer a solution to the operating speed limitation in electronics and the size limitation in photonics.

Surface Plasmon-Polaritons (SPPs) are TM polarized electromagnetic waves coupled to oscillations of electron plasma in a metal, propagating along the interface between two media with positive and negative permittivity, respectively. A thin metal film of finite width surrounded by a homogeneous dielectric can be used as a plasmonic waveguide supporting long-range SPP (LRSPP) which has low propagation loss and compatibility with the conventional photonic devices. Various plasmonic devices based on waveguides have been researched and plasmonic modulators also have been studied. Such devices can be used as a component in plasmonic integrated circuits.

The tunneling property of SPP across an interruption in Insulator-Metal-Insulator (IMI) typed slab waveguides embedded in a dielectric medium is investigated and discontinuous SPP waveguides with a gap (G-SPPWs) are suggested and demonstrated to control the guided SPP with external energy conveniently. The optimum structure for G-SPPWs in terms of the coupling and propagation losses are also researched.

Some research groups have presented the method of manipulating SPP using the control of free electrons inside a metal, e.g. electric current and magneto-optical effect. In this paper, we analyzed output SPP modes affected by polarized light across the gap in order to clarify the experimental observation which plasmonic signals are invertedly copied from an optical signal. The SPP mode characteristics and the propagation loss in the output SPPW were calculated with the G-SPPW and the dielectric channel waveguide for various cases

Kim, G., Koo, S. and Lee, M.
Analysis of Surface Plasmon-Polariton Modes with Metallic Structures and Polarized Light across Gapped Plasmonic Waveguides.
DOI: 10.5220/0009353201800184
In *Proceedings of the 8th International Conference on Photonics, Optics and Laser Technology (PHOTOPTICS 2020)*, pages 180-184
ISBN: 978-989-758-401-5; ISSN: 2184-4364

according to the polarization and the shape of the inserted metal strips.

The rest of this paper is organized as follows. First, we describe the design and simulation details for the mode analysis in Section 2. Section 3 presents the simulation results and discussion. In section 4, the conclusions are provided.

2 DESIGN AND SIMULATION DETAILS

Figure 1(a) shows the schematic diagram of a G-SPPW and a dielectric channel waveguide across the gap. The G-SPPW consists of the input and output IMI typed SPPWs with a gap. The gap length is set to be 8 μm since the coupling loss at the output SPPW begin to increase rapidly when the length is over 8 μm. The dielectric channel waveguide is laid across the gap and polarized light is launched to the dielectric channel waveguide. Gold was used as the metal of the SPPWs with 4 μm width and 20 nm thickness. The lengths of the input and output SPPWs are 10 μm and 14 μm, respectively. Low loss polymers were used as the 30 μm-thick upper and lower dielectric cladding layers and the core of the dielectric channel waveguide with 10 x 6 μm^2 cross-section, respectively. Figure 1(b) and (c) show schematic views from the *x*-*y* plane of horizontal and vertical gold strips in the gap. The horizontal strips, spaced about 1 μm, consist of two gold strips with 1 μm wid-

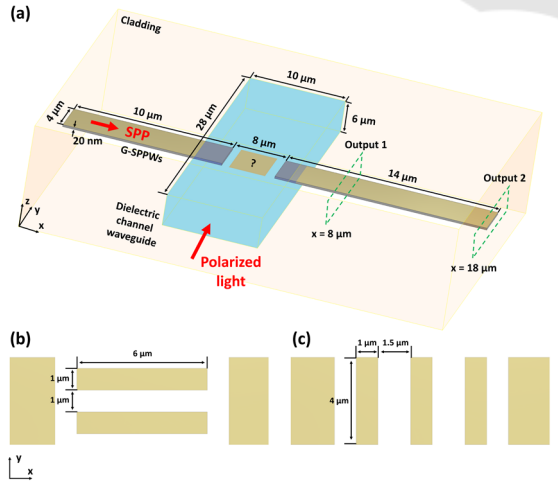

Figure 1: Schematic diagrams of simulated (a) G-SPPWs and dielectric channel waveguide and inserted 20 nm thick- (b) horizontal and (c) vertical gold strips.

th, 20 nm thickness and 6 μm length. The vertical strips, evenly spaced about 1.5 μm, consist of three gold strips with 1 μm width, 20 nm thickness and 4 μm length. The refractive indices of the gold for the SPPWs, the low loss polymer for the clad and the low loss polymer for the core are 0.550-11.4912i, 1.450 and 1.460 at a wavelength of 1.55 μm, respectively.

We used FDTD of Lumerical Inc. to solve Maxwell's equations in finite-difference time-domain method and calculated the SPP mode characteristics at the wavelength of 1.55 μm for optical communication applications. In the simulation, the mode source was used to excite a fundamental LRSPP mode in the input SPPW. The fundamental TE or TM mode source were used in the dielectric channel waveguide with the length of 28 μm. The SPP and polarized light intersect at the center of the gap. Perfectly matched layers were used in the 3-dimensional simulation space as a boundary condition to absorb electromagnetic waves incident to the layers, reducing unwanted reflection at the layers. To analyze the SPP mode characteristics in the output SPPW, we put two frequency-domain field monitors that collect the field profile across x = 8 μm (output 1) and 18 μm (output 2) plane, respectively.

3 RESULTS AND DISCUSSION

Figure 2(a) and (b) show the spatial distribution of the normal electric field component (E_z) and the mode profile at z = 30 nm of the input SPP mode. The upper and lower E_z distributions are spatially symmetric with respect to the z-axis as shown in Figure 2(a). The normal electric field component develops an extremum at the center of the top and bottom interfaces and the mode profile is very similar to that of the long-range ss_b^0 mode, which indicates the fundamental LRSPP mode was excited in the input SPPW.

We calculated the output SPP mode without strip when polarized light wasn't launched. Figure 3(a) shows the E_z distribution at output 1. Figure 3(b) shows the mode profile at z = 30 nm in output 1. Figu-

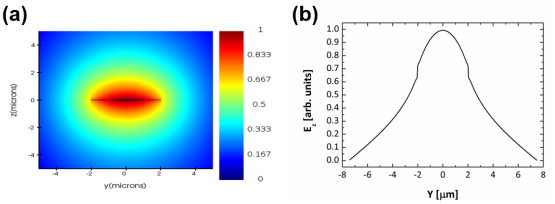

Figure 2: (a) E_z distribution and (b) mode profile at z = 30 nm of the input SPP mode.

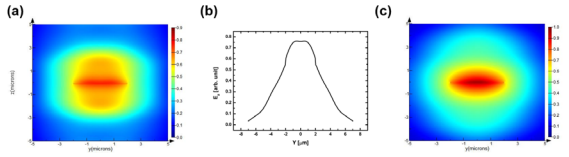

Figure 3: The output mode characteristics when polarized light isn't launched to the dielectric channel waveguide with no strip: (a) E_z distribution in output 1, (b) mode profile at z = 30 nm and (c) E_z distribution in output 2.

re 3(c) shows the E_z distribution at output 2. The SPP mode at output 1 is symmetric as shown in Figure 3(a) and the mode profile is also similar to that of the input SPP mode in Figure 2(a). As shown in Figure 3(c), the output SPP mode is maintained as it propagates along the output SPPW, which means that although there is a dielectric gap between the input and output SPPWs, the LRSPP is excited again in the output SPPW after the input SPP mode jumps over the gap.

Figure 4 shows the output SPP mode characteristics when SPP and TM polarized light propagate simultaneously along G-SPPWs without strip and the dielectric channel waveguide, respectively. Figure 4(a) shows the E_z distribution at output 1. Figure 4(b) shows the SPP mode profile at z = 30 nm (red line) in output 1. The black line represents the output SPP mode when the TM polarized light wasn't launched to the dielectric channel waveguide. The top and bottom output SPP modes are symmetric as shown in Figure 4(a) and there are mode fluctuations due to the E_z component of the TM polarized light. Figure 4(c) shows the E_z distribution at output 2 and indicates the fluctuating output SPP mode is stabilized as it propagates in the output SPPW.

Figure 5 shows the SPP mode characteristics at output 1 and 2 when SPP and TE polarized light propagate simultaneously along G-SPPWs without strip and the dielectric channel waveguide, respectively. The output SPP mode is affected by the TE polarized light even though the electric field of the TE polarized light oscillates along the x-axis and doesn't have the normal electric field component (E_z).

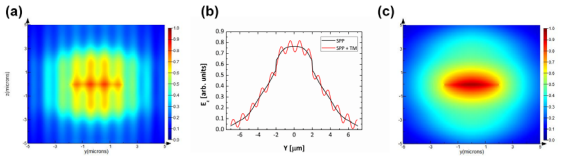

Figure 4: The output mode characteristics when the TM polarized light is launched to the dielectric channel waveguide with no strip: (a) E_z distribution in output 1, (b) mode profile at z = 30 nm and (c) E_z distribution in output 2.

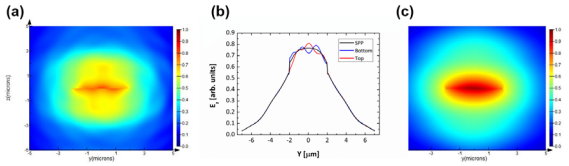

Figure 5: The output mode characteristics when the TE polarized light is launched to the dielectric channel waveguide with no strip: (a) E_z distribution in output 1, (b) mode profiles at $z = \pm$ 30 nm and (c) E_z distribution in output 2.

Figure 5(a) shows the E_z distribution at output 1. Figure 5(b) shows the SPP mode profiles at $z = \pm$ 30 nm (red and blue lines) in output 1. Top and bottom SPP modes (red and blue lines) are asymmetric and the intensity differences from the black line are opposite to each other, which denotes that the output SPP mode contains asymmetric short-range SPP (SRSPP) modes as well as the fundamental LRSPP mode. The electric field of SRSPP mode has a quite large loss because the fields are confined mainly into the metal and induces symmetric surface charge densities at top and bottom interfaces. The propagation length of SRSPP is limited to few microns. On the other hand, LRSPP mode has a low propagation loss and induces antisymmetric surface charge density at top and bottom interfaces, which is well matched with the absorption tendency of metallic nanoparticles according to the surface charge distribution. Figure 5(c) shows the E_z distribution at output 2 after 10 μm propagation from output 1. It is noticeable that the output SPP mode becomes the fundamental LRSPP mode again as it propagates in the output SPPW.

We also put horizontal and vertical gold strips in the gap to analyze whether metal structures inserted in the gap affect the output SPP mode. For the TM polarized light, there is no remarkable difference in the result of the case where the gold strips are not inserted, which reveals that SPP doesn't interact with TM polarized light which brings out antisymmetric surface charges like LRSPP. But for the TE polarized

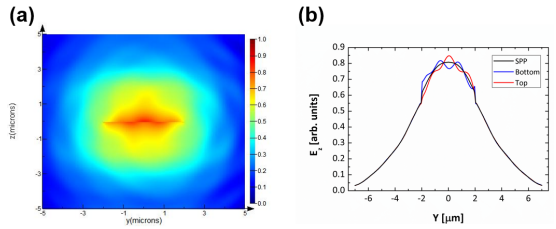

Figure 6: The output mode characteristics when the TE polarized light is launched to the dielectric channel waveguide with horizontal strips: (a) E_z distribution in output 1, (b) mode profiles at $z = \pm$ 30 nm.

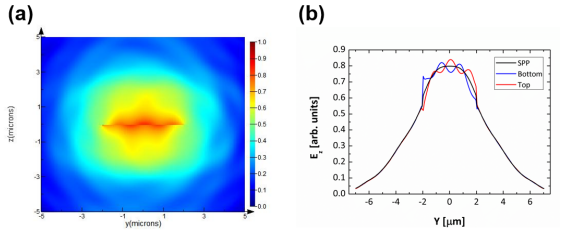

Figure 7: The output mode characteristics when the TE polarized light is launched to the dielectric channel waveguide with vertical strips: (a) E_z distribution in output 1, (b) mode profiles at $z = \pm 30$.

light, the output SPP mode profile is slightly different depending on the shape of gold strips. Figure 6 and 7 show the E_z distribution and mode profiles of the output SPP mode in output 1 when horizontal and vertical gold strips are inserted in the gap, respectively. The main difference between the two SPP mode profiles occurs near right and left edges ($y = \pm 2$ μm). For vertical strips, the top and bottom intensity differences from the black line are obviously larger than that of horizontal strips, which indicates that the electric field of the output SPP mode is more concentrated to the corner of the output SPPW than when horizontal strips are put in the gap. The fact that the more electric field of an SPP mode is concentrated at the corners represents the electric fields are highly confined inside the metal and fields at top and bottom interfaces are coupled weakly, resulting in a higher propagation loss.

To investigate the propagation characteristics of the output SPP mode for each simulated case, we calculated the propagation losses during 10 μm propagation from output 1 to output 2. As shown in Figure 8, when polarized light isn't launched without strip, the SPP mode propagates in the output SPPW with low attenuation of 0.0235 dB since the input SPP mode tunnels the gap and the LRSPP mode is re-excited in the output SPPW. The loss of the output SPP mode when the TM polarized light is launched to the dielectric waveguide with no strip is 0.0245 dB and very similar to that of the LRSPP, which signifies the LRSPP mode is maintained in the output SPPW without forming lossy SPP modes although there are mode fluctuations. The output SPP mode when the TE polarized light is applied without strip has a larger propagation loss of 0.0313 dB than the previous two cases. The difference in propagation loss arises from the radiation of higher-order SPP modes. Even though the gold strips are inserted into the gap, the loss is very similar to that of the LRSPP mode when the TM polarized light is applied. The loss increases when gold strips are put in the gap and the TE

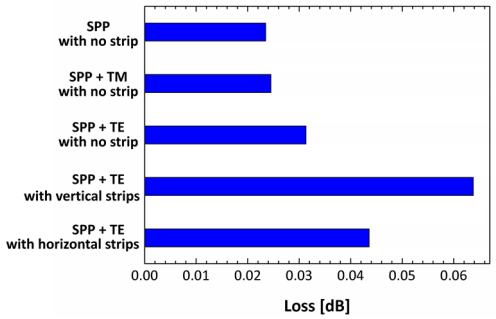

Figure 8: Comparison of the loss during 10 μm propagation from output 1 to output 2 for each case.

polarized light is launched to the dielectric channel waveguide. Especially when vertical strips are placed in the gap rather than horizontal strips, the loss increases significantly since the electric fields concentrated to the corners of output SPPW are confined inside the gold SPPW more, such SPP modes have a large propagation loss. The propagation losses when vertical and horizontal strips are put in the gap are 0.0638 and 0.0436 dB, respectively.

Only when the TE polarized light is launched to the dielectric channel waveguide, asymmetric higher-order SPP modes are excited and the propagation loss increases in the output SPPW, which implies that the TE polarized light across the gap can modulate the amplitude of SPP waves. As previous studies have shown, propagating SPP can be manipulated via the control of free electrons in the metal. The propagation loss of the output SPP mode increases since the surface charges induced by TE polarized light is symmetric with respect to the z-axis. When the metallic structures are put in the gap, the propagation loss in the output SPPW increases remarkably depending on the shape of the metallic structures as shown in Figure 8. Compared with horizontal strips, vertical strips have the more edges at which a polarized light induce surface charges. As symmetric surface charges are induced at metallic edges more, output SPP mode has more propagation loss. Given these results, TE polarized optical signals applied to the gap can invertedly generate modulated plasmonic signals from optical signals. Introducing metallic structures such as a photonic crystal in the gap will make the modulation depth much larger, resulting in a lowered modulating power.

4 CONCLUSIONS

We analyzed output SPP modes with the shape of gold structures inserted in the gap when polarized

light is launched to the dielectric channel waveguide laid across the gap. There is no significant effect on the output SPP mode when the TM polarized light is launched to the dielectric channel waveguide. Only when the TE polarized light is applied, lossy higher-order SPP modes are excited in the output SPP mode and the propagation loss increases remarkably depending on the shape of the gold strips, which suggests that modulating guided SPP mode is possible using the excited higher-order SPP modes. These phenomena can be applied to plasmonic signal generator in which plasmonic signals are invertedly generated from optical signals. Introducing metallic structures such as a photonic crystal in the gap will increase the modulation efficiency when plasmonic signals are copied from optical signals in the G-SPPWs.

ACKNOWLEDGEMENTS

This work was supported by the National Research Foundation of Korea (NRF) grant funded by the Korea government (MSIP) (No. NRF-2017R1A2B2009128).

REFERENCES

Koo, S.-R, Lee, D. H., Kim, G. and Lee, M.-H., 2019. Phenomena of copied plasmonic signals from optical signals. In *Rochester conference on coherence and quantum optics (CQO-11)*, Optical Society of America, p. M5A-2.

Gramotnev, D.K. and Bozhevolnyi, S.I., 2010. Plasmonics beyond the diffraction limit. *Nature Photonics*, 4, pp.83-91.

Ozbay, E., 2006. Plasmonics: merging photonics and electronics at nanoscale dimensions. *Science*, 311(5758), pp.189-193.

Zia, R., Schuller, J.A., Chardran, A. and Brongersma, M.L., 2006. Plasmonics: the next chip-scale technology. *Materials Today*, 9(7-8), pp.20-27.

Maier, S.A., 2007. Plasmonics: fundamentals and applications. Springer Science & Business Media.

Berini, P., 1999. Plasmon–polariton modes guided by a metal film of finite width. *Optics Letters*, 24(15), pp.1011-1013.

Lee, J.-M., Park, S., Kim, M.-S., Park, S.K., Kim, J.T., Choe, J.-S., Lee, W.-J., Lee, M.-H. and Ju, J.J., 2009. Low bending loss metal waveguide embedded in a free-standing multilayered polymer film. *Optics Express*, 17(1), pp.228-234.

Gacemi, D., Mangeney, J., Colombelli, R. and Degiron, A., 2013. Subwavelength metallic waveguides as a tool for extreme confinement of THz surface waves. *Scientific Reports*, 3, pp.1369.

Won, H.S., Kim, K.C., Song, S.H., Oh, C.H., Kim, P.S., Park, S. and Kim, S.I., 2006. Vertical coupling of long-range surface plasmon polaritons. *Applied physics letters*, 88(1), p.011110.

Park, H.-R., Park, J.-M., Kim, M.-S. and Lee, M.-H., 2012. A waveguide-typed plasmonic mode converter. *Optics Express*, 20(17), pp.18636-18645.

Cai, W., White, J.S. and Brongersma, M.L., 2009. Compact, high-speed and power-efficient electrooptic plasmonic modulators. *Nano Letters*, 9(12), pp.4403-4411.

Ayata, M., Fedoryshyn, Y., Heni, W., Baeuerle, B., Josten, A., Zahner, M., Koch, U., Salamin, Y., Hoessbacher, C., Haffner, C. and Elder, D.L., 2017. High-speed plasmonic modulator in a single metal layer. *Science*, 358(6363), pp.630-632.

Dicken, M.J., Sweatlock, L.A., Pacifici, D., Lezec, H.J., Bhattacharya, K. and Atwater, H.A., 2008. Electrooptic modulation in thin film barium titanate plasmonic interferometers. *Nano Letters*, 8(11), pp.4048-4052.

Dionne, J.A., Diest, K., Sweatlock, L.A. and Atwater, H.A., 2009. PlasMOStor: a metal-oxide-Si field effect plasmonic modulator. *Nano Letters*, 9(2), pp.897-902.

Sidorenko, S. and Martin, O.J., 2007. Resonant tunneling of surface plasmon-polaritons. *Optics Express*, 15(10), pp.6380-6388.

Lee, D.H. and Lee, M.-H., 2015. Gapped surface plasmon polariton waveguides for plasmonic signal modulation applications. *Journal of nanoscience and nanotechnology*, 15(10), pp.7679-7684.

Lee, D.H. and Lee, M.-H., 2019. Straight long-range surface plasmon polariton waveguides with a gap. *Journal of nanoscience and nanotechnology*, 19(10), pp.6106-6111.

Lee, D.H. and Lee, M.-H., 2016. Discontinuous tapered surface plasmon polariton waveguides with gap. *Journal of nanoscience and nanotechnology*, 16(6), pp.6275-6280.

Lee, D.H. and Lee, M.-H., 2019. Efficient experimental design of a long-range gapped surface plasmon polariton waveguide for plasmonic modulation applications. *IEEE Photonics Journal*, 11(1), pp.1-10.

Charbonneau, R., Scales, C., Breukelaar, I., Fafard, S., Lahoud, N., Mattiussi, G. and Berini, P., 2006. Passive integrated optics elements based on long-range surface plasmon polaritons. *Journal of Lightwave Technology*, 24(1), pp.477-494.

Berini, P., 2000. Plasmon-polariton waves guided by thin lossy metal films of finite width: Bound modes of symmetric structures. *Physical Review B*, 61(15), pp.10484-10503.

Bliokh, K. Y. and Rodriguez-Fortuño, F. J., 2018. Electric-current-induced unidirectional propagation of surface plasmon-polaritons. *Optics Letters*, 43(5), pp.963-966.

Hu, B., Wang, Q. J. and Zhang. Y., 2012. Broadly tunable one-way terahertz plasmonic waveguide based on nonreciprocal surface magneto plasmons. *Optics Letters*, 37(11), pp.1895-1897.

Palik, E.D., 1985. Handbook of Optical Constants of Solids. Orlando: Academic.

FDTD, Lumerical Inc. (https://www.lumerical.com).